Volume 1 | Number 1 | Jan 2013 | Pages 1–100

Journal of
Materials Chemistry A

Materials for energy and sustainability
www.rsc.org/materialsA

ROYAL SOCIETY
OF CHEMISTRY

ROYAL SOCIETY
OF CHEMISTRY

www.rsc.org/materialsA

Journal of Materials Chemistry A

ARTICLE

One step preparation of 'ready to use' Au@Pd nanoparticle modified surface using Deep eutectic solvents and a study of its electrocatalytic properties in methanol oxidation reaction.

Anu Renjith and V. Lakshminarayanan,

Deep eutectic solvents (DES) are being increasingly used in electrodeposition as it is considered as environmentally benign. We report here, a single step method for the preparation of Au-Pd core-shell nanoparticles (Au@Pd NPs) on a graphite rod in a DES medium. These ready to use mesoporous substrates were prepared by simultaneous electrodeposition of the insitu formed Au@Pd nanoparticles via anodic dissolution technique. The fabrication strategy by anodic dissolution in a DES avoided the addition of external stabilizers, reducing agents and metal salt precursors. The core-shell morphology of the nanoparticles was characterized by SEM while the elemental composition was confirmed by EDAX and cyclic voltametry. The catalytic characteristics of the Au@Pd nanoparticle modified graphite were systematically studied in the electrochemical oxidation of methanol by cyclic voltametry, Tafel analysis and activation energy measurements. The Au@Pd NPs exhibited superior catalytic performance over its corresponding monometallic counterparts viz., AuNPs and PdNPs prepared under identical conditions. The activation energy requirements of the Au@Pd NP modified graphite electrodes were low, making them a potential anode catalyst in alkaline media based methanol fuel cells at ambient temperatures. The method suggested here for the synthesis of mesoporous electrocatalysts is simple, effective and environmentally friendly.

Introduction

The advent of core shell nanoparticles has lead to a variety of applications, especially in the areas of biomedical devices, Li^+ ion storage, SERS, sensors and catalysts.[1-5] In the field of electrocatalyst, the recent studies are focused towards designing novel core-shell nanomaterials from proven catalytically active components. The conventional anode catalysts for the acid medium fuel cells were based on highly expensive and less abundant metal Pt. However, with the recent development in alkaline medium fuel cells (AFCs) owing to improved alcohol oxidation kinetics,[6] non Pt metals are being viewed as alternative catalyst materials. Efforts are also being made to decrease Pt loading in the catalysts by using Pt in combination with other metals. The metallic components studied for the design of core shell nanoparticles for AFC based electrocatalysts include Pd, which has a high catalytic activity in alkaline medium and Au, due to its higher tolerance to oxidative intermediates which act as poison in alcohol based fuel cells. Besides the additive effect of these catalytic components, the core-shell nanoparticles are also known to exhibit a synergistic effect due to the coupling of metals. There are several reports of the metallic components such as Pt, Pd and Au in combination with carbon supports such as carbon microspheres, carbon nanotubes, graphene which are

extensively studied for electrocatalytic applications in alcohol oxidation.[7-10]

The conventional methods of Au-Pd core shell nanoparticle synthesis (Au@Pd NPs) involve either galvanic replacement reaction or selective chemical reduction of the metal ions. These methods are based on the reduction of metal ions on the surface of a preformed metal core. The galvanic replacement method is based on the higher electrochemical reduction potential of gold over other metals such as Ag, Pt and Pd. This two step method involves the galvanic replacement of preformed nanoparticles of Ag or Co with gold giving hollow gold nanoparticles.[11-12] Through a second step, Pd is allowed to grow over the surface of these Au hollow nanoparticles giving Au@Pd NPs.

Recently, the electrochemical techniques are also employed for the deposition of bimetallic nanoparticles. Kim et al. performed an insitu formation and electrochemical deposition of bimetallic nanoparticles of Au and Pd. The deposited bimetallic nanoparticles were detached from the cathode and subsequently coated with gold shell to give PdAu@Au NPs.[13] Yang et al. electrodeposited Au@Pd nano composite on a carbon fibre by a two step potential pulse method from metal salt solutions.[14] Earlier, Reetz et al. had demonstrated the electrodeposition of nanostructured bimetallic clusters of Ni/Pd, Fe/Ni, Fe/Co onto a Pt sheet by the use of corresponding sacrificial anodes as metal sources.[15] However, the

nanoparticles obtained by the method did not exhibit a core-shell morphology. To the best of our knowledge, there are no reports on a single step electrochemical synthesis and *insitu* deposition of core-shell nanoparticles.

Chemical methods are also used for the preparation of Au@Pd NPs. A single step green synthesis of Au@Pd nanoparticles was achieved by utilizing the preferential reducing ability of plant tannins on Au ions over Pd.[16] Hu *et al.* carried out a seed mediated growth of palladium nanoparticles on the preformed nanoparticle of gold acting as a core.[17] Srivastava *et al.* succeeded in synthesizing Au@Pd nanoparticles by the simultaneous reduction of gold and palladium ions using tryptophan in aqueous medium.[18] Wu *et al.* synthesized Au@Pd NPs by co-reduction of corresponding metal salts in reverse miscellar solutions.[19] However, for electrochemical applications, all of these methods require additional steps to immobilize the prepared nanoparticles on to a suitable substrate. This may provide unstable surface and cannot with stand the harsh electrochemical environment in a cell.

In this study, we propose a facile single step fabrication of Au@Pd core-shell nanoparticles immobilized substrate which can be directly used for different applications. We used deep eutectic solvent, which is associated with adequate ionic conductivity and can be used as a standalone medium for the electrochemical process. The low surface tension of DES implies faster nucleation rates for nanoparticle formation.[20] The inherent reducing ability of ethylene glycol constituting the deep eutectic solvent (ethaline) avoids additional reducing agents. Besides, the components of DES viz., choline chloride and ethylene glycol are known to exhibit a stabilizing effect on the nanoparticles formed and hence avoids the addition of any external stabilizer.[21-22] The green aspects of DES were preserved by the choice of nanoparticle synthesis technique also as the anodic dissolution of Au and Pd wires avoids the addition of any metal ion sources. The process of electrodeposition ensures better adhesion of nanoparticles onto the substrate.

Experimental

Materials used

The components of DES, namely choline chloride and ethylene glycol (Fig.1a) were purchased from Aldrich and Merck respectively. Both of the DES components were kept in oven for 30 minutes to remove any traces of moisture. The metal wires of Au (0.5 mm diameter, 99.9%) and Pd (0.5 mm diameter, 99.9%) used for anodic dissolution were purchased from Advent Research Materials (U.K.). The electrochemical studies of the nanoparticle modified electrodes were performed using either sodium hydroxide or sulphuric acid (Merck) as supporting electrolytes in millipore water of 18MΩcm resistivity. Methanol (AR grade, Merck) was used for alcohol oxidation reaction.

Deep Eutectic Solvent (DES) preparation

Ethaline was used as the medium for the electrodeposition of nanoparticles. The preparation of ethaline was carried out by heating a mixture of choline chloride and ethylene glycol at a ratio of 1:2. The components were heated to 80° C under magnetic stirring till a homogeneous colorless liquid was formed.

Instrumentation

All the electrochemical experiments were performed using an EG&G potentiostat (model 263A) equipped with Powersuite software. The open circuit potential was measured prior to each experiment and was recorded by the software. The process of anodic dissolution and electrodeposition was carried out in a galvanostatic mode using a two electrode configuration while cyclic voltammetry and Tafel analysis were performed with a three electrode system. The electrochemical cell was maintained at specific temperatures for kinetic studies using Julabo temperature control systems (F25). For electroanalytical techniques, Pt foil was used as a counter electrode while the nanoparticle modified graphite rod was used as the working electrode. Saturated Calomel Electrode (SCE) and Hg/HgO/1M NaOH (MMO) were used as reference electrodes in acidic and alkaline medium respectively. SEM images and EDAX spectra were recorded with a field emission scanning electron microscope (Ultra plus, Carl Zeiss).

Electrodeposition of nanoparticles from DES

The metal wires of Au and Pd were used together as an anode for the electrodeposition of bimetallic nanoparticles. A graphite rod with a geometrical area of 0.19 cm^2 (circular base of the rod) was used as the cathode. The remaining area of the graphite exposed to the DES medium was sealed by Teflon (Fig.1b). The cathode and anode surfaces were kept parallel at a distance of 5 mm. The DES medium was kept at 50° C under constant magnetic stirring in an electrochemical cell of 10 mL capacity. The anodic dissolution and the simultaneous electrodeposition of bimetallic nanoparticles were carried out at a constant current density of 20 mA/cm^2 on Pd and 40 mA/cm^2 on Au in the ethaline medium for duration of 40 minutes. The variable current density on a single anode containing Au and Pd wires was achieved by exposing double the area of Pd wire *wrt* Au wire dipped in the solution.
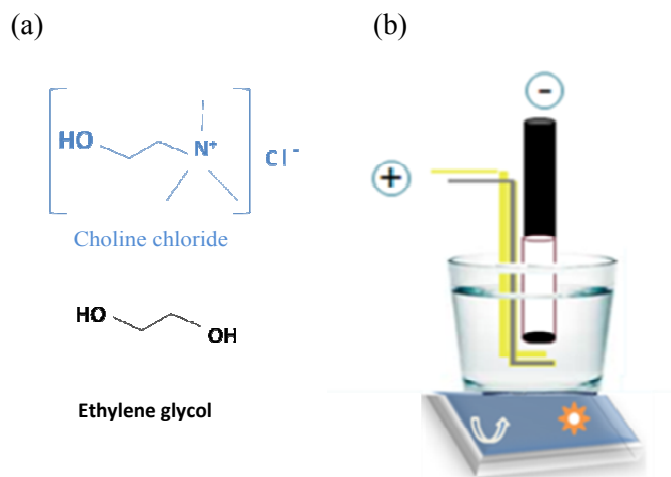
(a)   (b)

Fig.1. (a) Components of DES (b) Schematic representation of anodic dissolution technique for the electrodeposition of Au@Pd nanoparticle in DES medium

The electrodeposition of monometallic nanoparticles (Au and Pd) onto graphite was carried out at a current density (20 mA/cm^2) using the respective metal wire as the sacrificial anode. The amount of Pd dissolved in the medium was considerably higher than that of Au as calculated by the loss in weight of the anode (1 mg of Pd Vs ~0.2 mg of Au) after dissolution. The as prepared nanoparticle modified graphite rods were rinsed thoroughly with millipore water and dried prior to surface characterization and electrocatalytic studies.

Results and discussions

Voltammetric response of mesoporous substrates in acid medium

The cyclic voltammetry of the nanoparticle modified electrodes were carried out in 0.5 M H$_2$SO$_4$ at a scan rate of 100mV/sec in a scan range of -0.4 V to 1.3 V (Vs SCE). The cyclic voltammogram of Au NP modified graphite given in Fig.2a shows a broad peak in the anodic scan due to the formation of surface oxides of Au and the corresponding metal oxide stripping peak at 0.84 V during the cathodic scan.

Palladium is known for its ability to absorb hydrogen and this characteristic response of the mesoporous Pd electrode is apparent from Fig.2b. An intense anodic peak observed at ~ -0.1 V arises due to the oxidation of hydrogen absorbed within the lattice of mesoporous palladium. At potentials beyond 0.9 V palladium oxide is formed, which gets reduced at 0.26 V during the cathodic scan. The electrochemically active surface area (ECSA) of the mesoporous gold and palladium was calculated from the empirical charge densities associated with the stripping peak of AuO (390 μC/cm^2)[23] and that of PdO (424 μC/cm^2).[24] The large ECSA obtained for the monometallic nanoparticle modified substrates of gold (2.23 cm^2) and Pd (4 cm^2) compared to the geometrical area of graphite substrate (0.19 cm^2) pointed to the fact that nanoparticles are deposited as porous film of high surface area on the solid substrate.

Fig.2c shows the cyclic voltammogram of the Au@Pd film on a graphite substrate. The anodic scan shows the oxidation peak of absorbed hydrogen at around -0.05 V similar to that observed in the case of mesoporous Pd substrate. The first cathodic scan of Au@Pd nanoparticles manifests as a slightly broadened hump for the AuO→Au reduction while the sharp stripping peak corresponds to the reduction of PdO.

On successive scans of cyclic voltammograms, an increasing charge due to AuO reduction is observed with a concomitant decrease in the charge associated with PdO stripping peak. The decreased charge with electrochemical cycling is attributed to dissolution of PdO in acidic medium in presence of a more noble metal Au.[25] Deplanche *et al.* had earlier reported a similar observation on the Au@Pd core shell nanoparticles as a function of potential scanning.[26]

The presence of stripping peaks of both AuO and PdO in the voltammogram of Au@Pd NPs confirms the bimetallic nature of the mesoporous substrate. The reduction potentials of the surface oxides were shifted positive *wrt* their monometallic counterparts by 50mV. This shift in potential could be attributed to the interaction of the bimetallic components. The electro-deposition procedures followed in our studies involve simultaneous dissolution of the two metals, avoiding the requirement for a layer by layer deposition of the nanoparticles on the substrate. The fact that the stripping peak of gold oxide becomes apparent only after the simultaneous removal of palladium is an electrochemical evidence for the core-shell nature of the nanoparticles with Au constituting the core and Pd, the shell layer.

To probe into the morphological features of the electrodeposited nanoparticle modified substrate, SEM images were acquired. Fig.3 shows the SEM images and EDAX of the nanoparticle modified graphite prepared under identical experimental conditions. The SEM images of the mesoporous Pd substrate (Fig.3a) shows large clusters of nanoparticles with sizes varying from 10-20 nm. The surface distribution of these clusters is inhomogeneous which leads to the formation of numerous voids on the surface. These voids make the modified surface highly mesoporous [Fig.S1 of supporting information]. Fig.3b shows the surface of graphite extensively covered with gold nanoparticles of size ~50-70nm. In comparison to monometallic nanoparticle modified substrate, the coverage of Au@Pd nanoparticle on the surface of graphite was scattered. The SEM image of the electrodeposited bimetallic nanoparticles [Fig.3c] shows a brighter metallic component buried within another component, indicative of core-shell morphology. However, an EDAX analysis on the as prepared samples given in Fig.3d indicated the complete absence of gold in the regions scanned. The Pd composition was contributing 47 % (weight %) of the total composition comprising Pd, C and Cl. The elemental composition of the bimetallic nanoparticle on graphite is provided in Table S1 (supporting information).
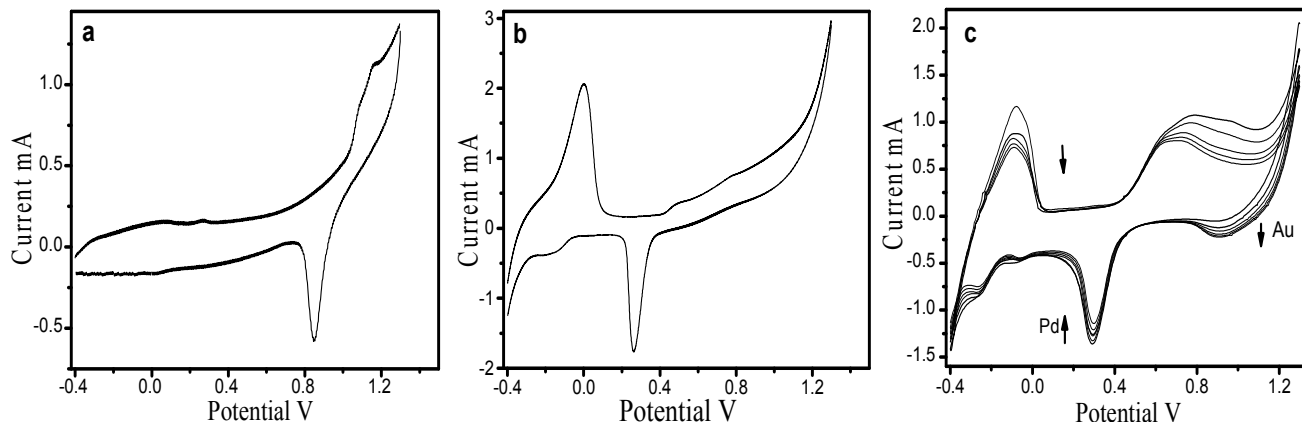

Fig.2. Cyclic voltammograms of graphite rod modified with nanoparticles of (a) Au (b) Pd (c) Au@Pd in 0.5M H$_2$SO$_4$ at a scan rate of 100mV/sec Vs SCE
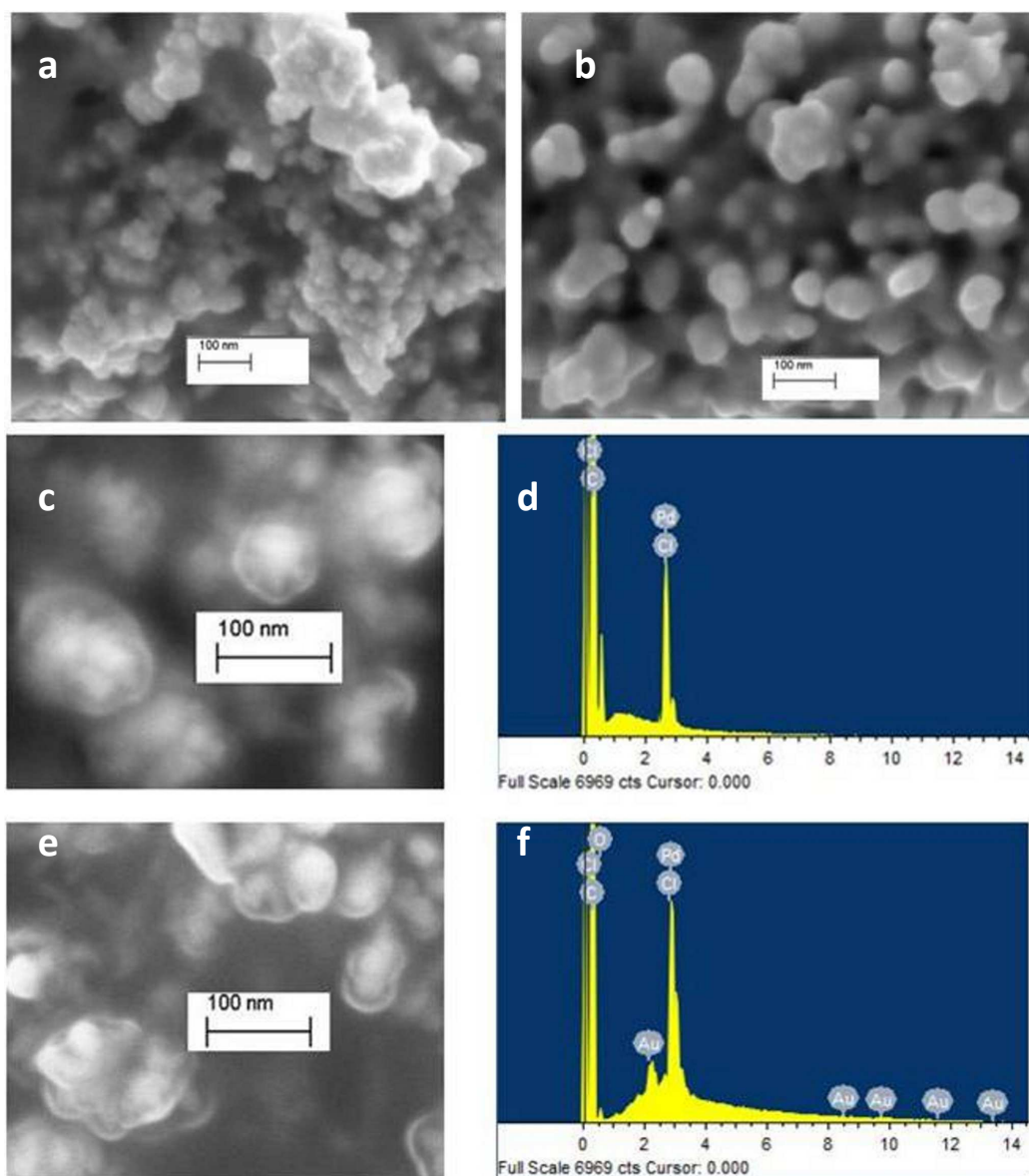
Fig.3. SEM images of graphite rod modified with (a) Pd (b) Au (c) Au@Pd NPs (d) EDAX of Au@Pd NPs (e) SEM images (f) EDAX of Au@Pd NPs on graphite after electrochemical treatment

The morphological analysis of the as prepared samples was compared with that of the samples subjected to electrochemical potential scanning (50 cycles). The SEM images of the electrochemically treated substrate given in Fig.3e revealed a decrease in particle size with the core – shell morphology being preserved. The EDAX spectrum of the substrate after electrochemical treatment shows the presence of gold [Fig.3f]. The elemental analysis of the electrochemically treated sample provided in Table S2 (supporting information) showed a decrease in the composition of Pd from 47% to 35%. The decrease in the composition of Pd with that of the corresponding increase in gold (0% to 2.64%) was in accordance with the behavior exhibited in the cyclic voltammogram (Fig.2c). The electrochemical analysis together with the morphological characterization confirms the presence of Au@Pd core-shell nanoparticles on the surface of graphite.

The mechanism of electrochemical formation of Au@Pd nanoparticles on the surface of graphite can be described as follows; The application of a constant current density at sacrificial anodes, releases metal ions of Au and Pd to the DES medium. The Pd wire dissolution was observed to be considerably higher than that of Au leading to an increased concentration of Pd ions in the medium. These metals ions instantaneously form complexes with the hydrogen bonded DES components.[22] The standard reduction potentials indicate that the electrochemical reduction of $AuCl_4^-$ is favored over $PdCl_4^-$ (1 V Vs 0.63 V).[19] Subsequently, the gold atoms associated with higher nucleation rates acts as a nucleic centre for the growth of nanostructured Pd layers. Higher nucleation rate of gold atoms over Pd has been reported earlier in aqueous[27] and reverse miscellar media.[19] An increased concentration of Pd ions in the medium causes deposition of

several layers of PdNPs on the gold nuclei, which probably accounts for the absence of gold in the EDAX elemental analysis of the as prepared substrate.[28-29] However, gold is shown up by EDAX analysis only after the Pd atoms from the shell of the nanoparticles are electrochemically etched and gold atoms are exposed. EDAX line scan of the electrochemically etched Au@Pd NPs is provided in Fig.S2 of supporting information.

Chirea *et al.* synthesized gold nanowires chemically in ethaline medium using an external reducing agent $NaBH_4$.[22] The method required excessive amount of $NaBH_4$ for the reduction of the gold - ethaline complex [HO-CH_2-CH_2-$N^+(CH_3)_3$]$AuCl_4^-$.2(HO-CH_2-CH_2OH). This observation points towards the fact that the DES medium by itself cannot reduce the gold complexes to yield AuNPs in the solution. It therefore indicates that, in our studies the AuNPs could have been formed by the electrochemical reduction of the complex on the surface of the cathode. However, the synthesis of palladium nanoparticles utilizing the reducing ability of alcohols especially ethylene glycol have already been studied in detail.[30-31] The ethaline medium comprising of choline chloride and ethylene glycol are weakly bound, increasing the chances of chemical reduction of Pd ions in addition to the electrochemical reduction. The reducing ability of the medium brings about the formation of PdNPs in the DES medium making the color of the medium turn dark, as observed in our experiment.

Enhanced catalytic activity of Au@Pd bimetallic nanoparticle over monometallic analogues

The electrocatalytic activity of the Au@Pd nanoparticles on graphite was investigated in methanol oxidation in alkaline medium and compared with that of its monometallic counterparts. The electro-oxidation of alcohols largely depends on the coverage of hydroxyl ions adsorbed on the surface of the catalyst from the alkaline medium. However, an optimum control of hydroxyl ion concentration is necessary to ensure the accessibility of electro-active sites for the reactant alcohol molecules and the concentration of NaOH was maintained at 0.5 M in this study. The currents reported here for the electro-oxidation of methanol using the mesoporous substrates were normalized to ECSA and hence can be attributed to the catalytic activity and not to the higher surface area.

Electro-oxidation of methanol in alkaline medium

The electrocatalytic properties in terms of current density and overpotential of the modified electrodes for methanol oxidation were studied by cyclic voltametry. A synergistic effect of Au and Pd, if any was examined by the comparison of voltammetric response of Au@Pd nanoparticle with that of its monometallic counterparts.

The cyclic voltammogram of the mesoporous gold substrate given in Fig.4a displays a small hump (-0.1 V) in the anodic scan prior to the intense oxidation peak. The methanol oxidation on gold in alkaline media is known to be occurring at two potential regions. The reaction mechanism on polycrystalline gold in alkaline medium was earlier investigated by Borkowska *et al.*[32] They obtained two peaks with the first peak at negative potentials being attributed to the oxidation of methanol on hydroxyl ion adsorbed gold surface to yield formate ions releasing four electrons in the process.

$$CH_3OH + 5OH^- \rightarrow HCOO^- + 4H_2O + 4e^-$$

At higher potentials, methanol oxidation proceeds on the surface of gold oxide which results in the formation of carbonates releasing six electrons in the process. The group has confirmed the independent reactions of methanol oxidation on gold hydroxide and gold oxide surfaces by Tafel slope analysis.

$$CH_3OH + 8OH^- \rightarrow CO_3^{2-} + 6H_2O + 6e^-$$
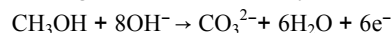
The cyclic voltammograms of methanol oxidation on mesoporous palladium substrate shown in Fig.4b displays a single peak at low overpotentials compared to gold. The palladium based substrates have been known to render superior electrocatalytic activities in alkaline medium based direct alcohol fuel cells. The electro-oxidation of methanol on palladium based catalysts yields formate as the main product which was by confirmed by HPLC.[33] However, ex-situ analytical studies of anode exhaust of methanol oxidation catalyzed by Pd based materials have confirmed the presence of carbonates also along with formates.[6]

Fig.4c shows the voltammograms displaying the methanol oxidation on mesoporous Au@Pd modified graphite. The voltammograms exhibit similar features to that of the PdNP modified substrates. The Au@Pd bimetallic substrate shows a single peak in the anodic scan unlike that observed on the
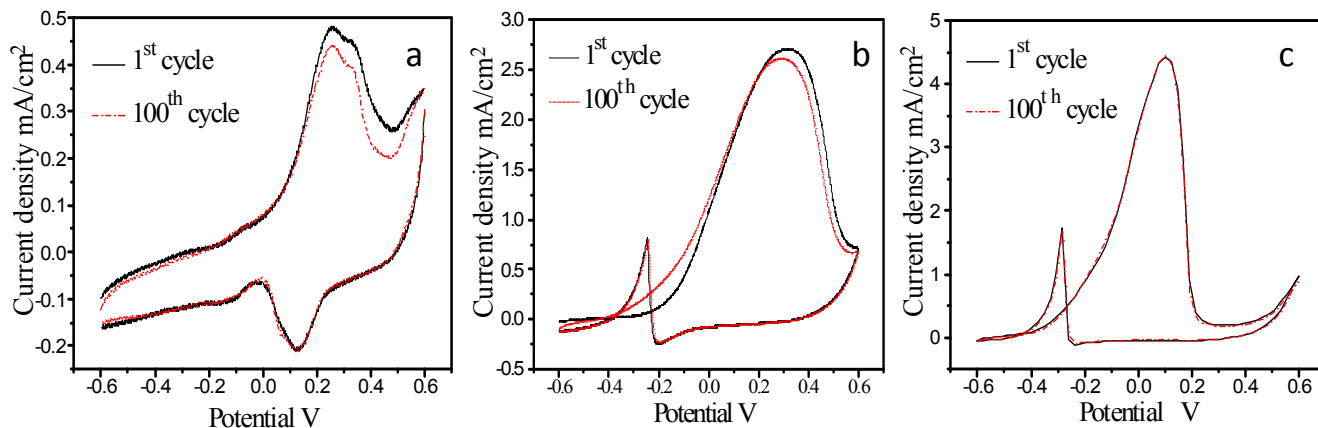

Fig.4. Cyclic voltammograms of graphite rod modified with nanoparticles of (a) Au (b) Pd (c) Au@Pd in 2M MeOH / 0.5M NaOH at a scan rate of 100mV/sec (Vs MMO)

AuNP modified substrate. This may be ascribed to the fact that the Au core is well buried within Pd shells and the electro-active sites of the latter are more accessible for the reactant molecules. A synergistic effect of bimetallic components of Au@Pd modified substrates is evident on the comparison of peak potentials and current densities with that of monometallic counterparts.

Previously Song *et al.* prepared hollow Au@Pd NPs based electrocatalyst by adhering chemically formed Au@Pd nanoparticles on a glassy carbon electrode by means of Nafion.[11] The study showed that the electrocatalytic properties of Au@Pd in ethanol oxidation were superior to that of Au@Pt prepared under identical conditions. A comparison of the electrocatalytic properties of hollow Au@Pd, Au and Pd nanoparticles on a glassy carbon electrode by Liu *et al.* indicated that the Au@Pd hollow nanostructures exhibited better catalytic activity in terms of current density (0.6mA/cm^2) at a peak potential of -0.12V Vs Ag/AgCl for a methanol concentration of 0.5M at a scan rate of 50mV/sec.[12] Su *et al.* prepared bimetallic nanoparticles of Au and Pd immobilized onto carbon rods in various compositions and were used as catalysts in the electro-oxidation of methanol, ethanol and isopropanol[34]

At a concentration of 1M, the methanol oxidation currents were in the range of 30 - 42mA/cm^2 (wrt geometrical area) for different Au:Pd compositions. The study showed that the stability and poisoning tolerance of Pd was not significantly enhanced by the presence of Au. Lang *et al.* prepared nanoporous substrates of AuPd by a dealloying process and showed that the electrodes displayed high electrocatalytic properties for methanol oxidation (0.4mA/cm^2 at a peak potential of 0.21V Vs Ag/AgCl).[35]

In our studies, the electrodeposited Au@Pd core shell nanoparticle exhibited enhanced catalytic properties in terms of a current density of 4.5mA/cm^2 normalized to ECSA (74 mA/cm^2 *wrt* geometrical area) at a peak potential of 76mV (Vs

Table 1: Comparison of open circuit (E$_{OCP}$), onset (E$_{Onset}$), peak (E$_{Peak}$) potentials graphite rod modified with nanoparticles of Au, Pd and Au@Pd with literature values.[32,36,37]

	E $_{OCP}$ (V)	E $_{Onset}$ (V)	E $_{Peak}$ (V)
AuNP	0.754	0.835	1.131
PdNP	0.516	0.555	1.152
Au@Pd NP	0.441	0.450	0.935
Pt-C/GC ^{A}	-	0.412	0.92
Pt/GC ^{B}	-	0.443	1
Pt/Ru ^{C}	-	0.333	0.914
Pt disc	-	0.4	1

A-chemical deposition of commercial Pt catalyst on glassy carbon, B-electrochemical deposition of commercial Pt catalyst on glassy carbon, C- Pt/Ru catalyst on high surface area carbon

MMO). Table 1 shows the open circuit (E$_{OCP}$), onset (E$_{Onset}$), peak (E$_{Peak}$) potentials for the three different electrodes studied in this work. It can be seen that the methanol oxidation onset potential and open circuit potentials are quite close in all the cases. This shows that negligible overpotential (40 mV) is required in the case of Pd nanoparticles electrodes whereas the onset potentials are almost matching the OCP in the case of Au@Pd. The onset and peak potentials for methanol oxidation on Au@Pd NP catalysts are comparable to the state of the art electrocatalysts (Pt and Pt-Ru) for methanol electro-oxidation.

The stability of nanoparticle modified graphite electrodes (AuNP, PdNP and Au@PdNP) was monitored with continuous potential scans in 2M methanol / 0.5M NaOH. The Au@Pd nanoparticle modified electrodes were extremely stable to methanol oxidation over continuous scans [Fig.4c]. The stability of monometallic counterparts is also apparent from the Figures 4a and 4b.

During the reverse scan, a reduction peak of very low current can be observed at ~ -0.23 V followed by a sharp oxidation peak as in Fig.4b and Fig.4c. The reduction peak corresponds to the stripping peak of PdO similar to that seen earlier in 0.5M H$_2$SO$_4$ (Fig.2b). The negative shift in the potential of stripping peak is attributed to the change in the pH of the medium from acidic to alkaline. Such an electrochemical reduction of PdO during the cathodic scan creates fresh Pd atoms that lack lattice stabilization and thereafter are not in equilibrium with the lattice.[38-39] These non-equilibrated Pd atoms are associated with high catalytic activity. Interestingly the Au@Pd NPs associated with Pd shells displayed similar behavior as that of PdNPs.

Manoharan *et al.* studied the changes associated with the reverse oxidation peak current (I$_p$) of alcohol oxidation on Pt in acidic medium on scanning to high anodic limits.[40] It was observed that this current decreased on extending the anodic limits. It is known that at potentials beyond 1.3V, removal of carbonaceous species via evolution of CO$_2$ occurs.[41] Such a decrease in peak current confirms that the reverse oxidation peak current is associated with oxidation of residual carbon species of alcohol. Recent studies of alcohol oxidation in alkaline medium on metals such as Pt, Pd are also attributed reverse anodic peak to the same phenomenon.[10,34,42]

The reverse anodic peak can be also explained in terms of catalytic activity of freshly reduced metal sites. The oxidation peak at -0.3V in the cathodic scan immediately after the stripping peak is due to the methanol oxidation occurring on the surface of freshly prepared Pd atoms as explained by Manzanares *et al.* in the electro-oxidation of formic acid on Palladium in acidic medium.[43]

In our studies, Pd shell of Au@Pd NP provides catalytic sites for the electro-oxidation of methanol as discussed in previous section. Therefore, we have also studied PdNP modified graphite electrode for the cyclic voltammetric experiments. Fig.5a shows the cyclic voltammogram of PdNP modified graphite in 0.5M NaOH. Pd oxide formation and stripping peak of PdO is evident in the anodic and cathodic scan respectively. In the presence of 2M methanol (Fig.5b), an intense methanol oxidation peak can be seen during the forward scan and also a anodic peak in the reverse scan. To confirm whether the reverse anodic peak is indeed due to the adsorbed carbonaceous species, the oxidation process was stopped and reversed at the peak potential associated with maximum extent of the methanol oxidation. This would ensure that the carbonaceous impurities are retained on the surface and can undergo oxidation during

the reverse scan. However, counter-intuitively no reverse anodic peak was observed as apparent in Fig.5c. Another experiment of extending anodic limit to 1.3V, resulted in a substantial decrease in reverse anodic peak current (Fig.5d), similar to that observed by Manoharan *et al.*.[40] It is evident therefore, that oxidation of residual carbonaceous impurities can occur only in the presence of freshly formed Pd atoms. This is also confirmed from Fig.5c, where on restricting the anodic limit to E_p no stripping peak is observed which indicates that fresh Pd atoms are not formed and residual carbon species do not get oxidized during cathodic scan. Earlier Takamura *et al.* studied the adsorption and oxidation of methanol on Palladium in alkaline medium by specular reflectivity.[44] The reverse anodic peak was attributed to electro oxidation of organic entities on freshly formed Pd sites as confirmed by our observation.
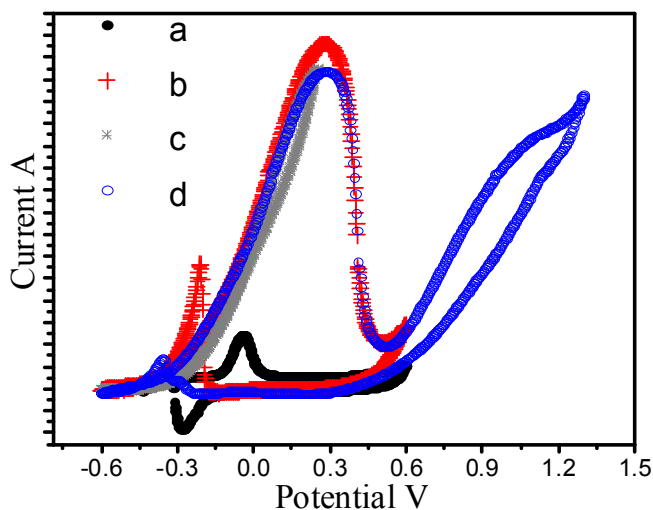

Fig.5. Cyclic voltammograms of graphite rod modified with Pd NPs in (a) 0M MeOH (b) 2M MeOH, anodic limit 0.6 V (c) 2M MeOH, anodic limit 0.255 V (d) 2M MeOH, anodic limit 1.3 V at a scan rate of 100mV/sec in 0.5M NaOH (Vs MMO)

Kinetics of methanol electro-oxidation

The data obtained from the voltammetric response of nanoparticle modified electrodes towards methanol oxidation reaction were subjected to a detailed kinetic analysis based on Tafel analysis, activation energy measurements and reaction order calculations.

Tafel analysis

Tafel analysis is usually done to get insight into the rate determining step. However in the case of alcohol oxidation, Tafel slopes often show large deviations from ideal values owing to undesired reactions of adsorbed reactive intermediates and excessive coverage of poisoning species on catalytic surface. The decomposition of methanol to CO on Pd in gas phase was studied by Davis *et al.*[45] The group suggested that methanol adsorption on to the metal site occurs through the oxygen atom which subsequently forms an adsorbed methoxy intermediate. The rate determining step in the decomposition of methoxy intermediate to carbonyl species was the cleavage of –C-H bond. There are several studies on the mechanism of methanol oxidation on Pt in acidic and alkaline media, Au in alkaline medium, MoO_3 in gas phase.[46-49] The sequence of

reaction steps proposed was somewhat different in each of these cases. Nevertheless, in all of these systems, the rate determining step was proposed as the –C–H bond scission as in the following reaction, whch yields a Tafel slope of 120mV/dec in the i-V curve.

$$CH_3OH \rightarrow *CH_2OH + H^+ + e^-$$

Recently, Kwon *et al.* studied the mechanism of electro-oxidation of alcohol in alkaline media by establishing the Hammett relationship.[50] Though the studies were performed on a gold surface, the implications of the model could be applied for Pt and Pd based catalyst in alkaline media. The proposed two step pathway involves an initial deprotonation of methanol resulting in an alkoxide ion. This is followed by a second deprotonation step as discussed above to give an aldehyde. The initial deprotonation is base catalyzed while the second deprotonation is characteristic of the electrode material.

In our studies, Tafel analysis was performed by conducting chronoamperometry at various potentials at the foot of the methanol oxidation peak (obtained from cyclic voltametry) at different temperatures. The Tafel plot for the methanol oxidation catalyzed by the Au@Pd NPs is provided in Fig.6. The Au@Pd nanoparticle modified graphite exhibit Tafel slopes varying from 122 to 135 mV/dec at a temperature range of 288K-308K. The obtained results are in agreement with the theoretical prediction of 120mV/dec for an electrochemical reaction involving a single electron transfer during the rate determining step. The values were comparable with the Tafel slopes obtained for methanol oxidation on carbon supported Pt/Ru catalyst at a similar temperature range.[51]
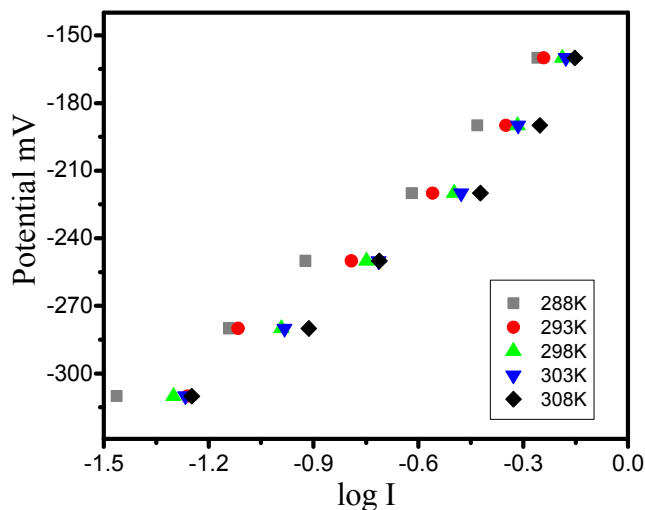

Fig.6. Tafel plots of Au@Pd NP modified graphite rod in 2M MeOH / 0.5M NaOH Vs MMO at different temperatures

The Tafel slopes obtained for all the mesoporous substrates under study are provided in Table 2. Tafel slopes obtained for mesoporous substrates of gold and Pd show deviations from the ideal value of 120 mV. These deviations are attributed to the oxidative intermediates that get adsorbed on to electrode surface and prevent the accessibility of fresh reactant molecules onto the catalytically active sites.[47] Such a reduced accessibility would necessitate excess applied potential to maintain the same defined current. Thus, in general a high Tafel slope, $d\eta$ /d(log i)

hints at the surface contamination owing to the adsorption of intermediates of methanol oxidation. The Tafel plots for methanol oxidation catalyzed by AuNP and PdNP modified monometallic graphite are provided in Fig.S3 a and b respectively of supporting information. It is evident from the table that the Au@Pd NPs are associated with better tolerance to poisoning intermediates. Thus, the catalytic sites are accessible to fresh methanol molecules maintaining the Tafel slopes close to the predicted values.

Table 2: Tafel slopes for methanol oxidation on AuNP, PdNP and Au@Pd NPs at various temperatures

Temperature (K)	Tafel slopes (mV/dec)		
	AuNP	PdNP	**Au@PdNP**
288	241	178	**122**
293	170	163	**135**
298	214	171	**131**
303	203	178	**134**
308	221	193	**131**

Activation energy measurements

The activation energy for an electrochemical process is a measure of the catalytic efficiency. Higher activation energy necessitates higher operating temperatures for methanol oxidation. The activation energy (E_a) for the electro-oxidation of methanol was determined from the Arrhenius plot of log I Vs T^{-1} at low overpotential regions. Ea was obtained by equating the slope of the linear fit of the Arrhenius plot to $-Ea/2.303R$, R being gas constant. The activation energy plots, as expected show an increase in log I with temperature at any overpotential studied. Such an increase in log I with temperature is attributed to the enhanced adsorption of hydroxyl ions from the alkaline medium, which provides active oxygen species required for electro-catalysis.[52] In an alkaline medium, Pd based catalysts are known to lower the activation energy for methanol oxidations much more than that of Pt/Ru electrocatalyst (40-50 kJ/mol) and are extensively studied as Pt alternative.[53] The activation energy required for methanol oxidation on a Pd disc electrode was studied by Wang *et al.* in alkaline medium and was found to be ~33 kJ/mol.[42] Recently, for methanol oxidation reaction, the Pd-Ni-Cu-P metallic glass nanowire catalyst in an alkaline media showed improved poisoning resistance and lowered onset potential.[54] The activation energy required for the electro-oxidation process was found to be 22 kJ/mol.

The Arrhenius plots for monometallic substrates of PdNP and AuNP modified graphite rods in our studies at different overpotentials are provided in Fig.S4 a and b of supporting information. The PdNP modified graphite rod exhibited an average Ea of 22.5kJ/mol. However, Ea requirement for

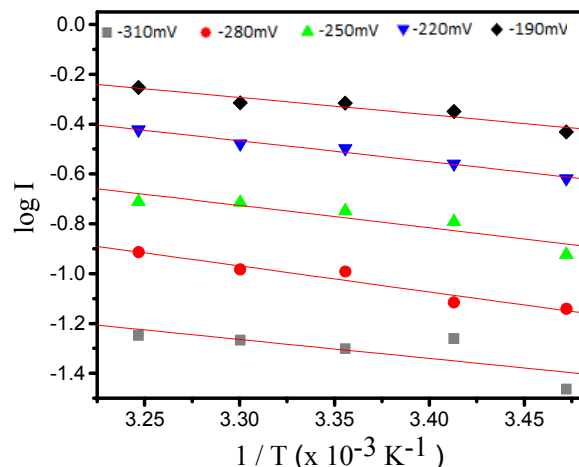methanol electro-oxidation on gold nanoparticle modified graphite (~27 kJ/mol) was somewhat higher than that of Pd.

Fig.7. Arrhenius plots for Au@Pd nanoparticle modified graphite rod in 2M MeOH / 0.5M NaOH Vs MMO at different potential ranges

An enhanced performance of Au@Pd modified substrate is evident from the very low activation energies (13 – 20 kJ/mol) at a potential range of -0.310 V to -0.160 V giving an average Ea of 16.2 kJ/mol. The Arrhenius plots obtained for the process are provided in Fig.7. The synergistic catalytic effect for Au and Pd is evident from the very low activation energies for methanol oxidation when compared to their monometallic counterparts and also to other catalytic materials reported in literature.

Reaction order calculations

The reaction order of the methanol oxidation on Au@Pd NPs was calculated from the plot of log I Vs log C by the equation, log I = log nFk + m logC, where F is the Faraday constant, k is the reaction constant, m is the reaction order and C is the concentration of alcohol. A Linear relationship obtained [Fig.8] indicates that the mechanism involved is not affected by the concentration of the reactant.
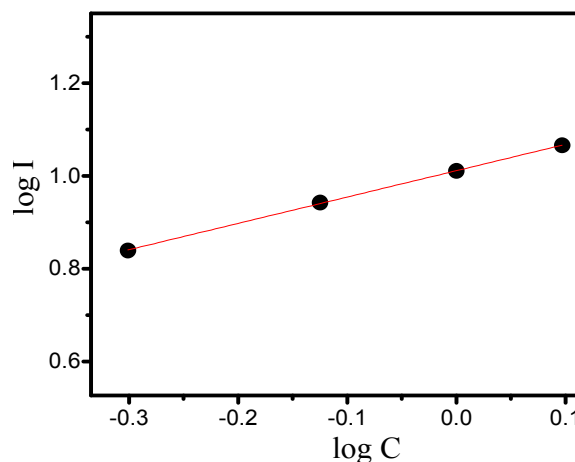

Fig.8. log C Vs log I plots for electrochemical oxidation of methanol catalysed by Au@Pd NPs at peak potential

The slope of 0.56 at peak potential (70 mV) indicates that the reaction order is ½ similar to that of Pt in acidic and alkaline media.[30,49,37]

Conclusions

Robust nanostructures of Au@Pd, Au and Pd nanoparticles were synthesized via novel electrochemical route in a deep eutectic solvent. The method exploits the stabilizing effect of the DES components. The material requirements for the proposed nanoparticle synthesis are minimal and totally eco-friendly. The electrodeposited films were well adherent and stable for continuous electrochemical treatment at varying temperatures and are expected to better than electrocatalysts modified in dispersing medium like Nafion. The fabricated nanoparticle modified substrates were extensively studied as electrocatalyst for methanol oxidation in alkaline media. The Au@Pd nanoparticles modified substrates displayed superior performance over their monometallic counterparts in terms of voltammetric response and high CO poisoning tolerance. The Arrhenius plots reveal markedly low activation energy requirements for the Au@Pd NPs. The material developed here can be deposited on any conducting substrate and hence can be utilized as potential candidates for fuel cell applications.

Acknowledgements

Address

Soft Condensed Matter Group,

*Raman Research Institute,*

Bangalore- 560080, India.

References

1. Z. Fan, D. Senapati, A. K. Singh and P.C. Ray, *Mol. Pharmaceutics*, 2013, **10**, 857.

2. Y. Park, S.Yoo and S. Park, *Langmuir,* 2008, **24**, 4370.

3. D. Deng and J. Y. Lee, *Chem. Mater.*, 2008, **20**, 1841.

4. S. Guha, S. Roy and A. Banerjee, *Langmuir*, 2011, **27**, 13198.

5. H. Shin and S. Huh, *ACS Appl. Mater. Interfaces*, 2012, **4**, 6324.

6. C. Bianchini and P. K. Shen, *Chem. Rev.,* 2009, **109**, 4183.

7. L. D. Zhu, T.S. Zhao, J. B. Xu and Z. X. Liang, *J. Power Sources,* 2009, **187**, 80.

8. C. Xu, L. Cheng, P. Shen and Y. Liu, *Electrochem. Commun.,* 2007, **9**, 997.

9. D. F. Silva, A. N. Geraldes, E. Z.Cardoso, M. M. Tusi, M. Linardi, E. V. Spinacé and A. O. Neto, *Int. J. Electrochem Sci.,* 2011, **6**, 3594.

10. M. Zhang, Z. Yan, Q. Sun, J. Xie and J. Jing, *New J. Chem.*, 2012, **36**, 2533.

11. H. M. Song, D. H. Anjum, R. Sougrat, M. N. Hedhilib and N. M. Khashab, *J. Mater. Chem*., 2012, **22**, 25003.

12. Z. Liu, B. Zhao, C. Guo, Y. Sun, F. Xu, H. Yang and Z. Li, *J. Phys. Chem. C,* 2009, **113**, 16766.

13. M. J. Kim, K. J. Park, T. Lim, S. Choe, T. Yu and J. J. Kim, *J. Electrochem. Soc.,* 2013, **160**, E1.

14. F. Yang, K. Cheng, T. Wu, Y. Zhang, J. Yin, G. Wang and D. Cao, *Electrochim. Acta*, 2013, **99**, 54.

15. M. T. Reetz, W. Helbig and S. A. Quaiser, *Chem. Mater.*, 1995, **7**, 2227.

16. X. Huang, H. Wu, S. Pu, W. Zhang, X. Liao and B. Shi, *Green Chem*., 2011,**13**, 950.

17. J. Hu, Y. Zhang, J. Li, Z. Liu, B. Ren, S. Sun, Z. Tian and T. Lian, *Chem.phys.Lett.*, 2005, **408**, 354.

18. S. K. Srivastava, T. Hasegawa, R. Yamada, C. Ogino, M. Mizuhata and A. Kondo, *RSC Adv.*, 2013, **3**, 18367.

19. M. Wu, D. Chen and T. Huang, *Langmuir,* 2001, **17**, 3877.

20. K. Richter, P.S. Campbell, T. Baecker, A. Schimitzek, D. Yaprak and A. Mudring, *Phys. Status Solidi B,* 2013*,* **250**, 1152.

21. L. Wei, Y. Fan, N. Tian, Z. Zhou, X. Zhao, B. Mao and S. Sun, *J. Phys. Chem. C*, 2012, **116**, 2040.

22. M. Chirea, A. Freitas, B. S. Vasile, C. Ghitulica, C. M. Pereira and F. Silva, *Langmuir*, 2011, **27**, 3906.

23. S. Trasatti and O. A. Petrii, *Pure & Appl. Chem.*, 1991, **63**, 711.

24. W. Pan, X. Zhang, H. Ma and J. Zhang*, J. Phys. Chem. C,* 2008, **112**, 2456.

25. K. Juodkazisz, J. Juodkazyt , B. Sebeka, G. Stalnionis, and A. Lukinskas, *Russian Journal of Electrochemistry*, 2003, **39**, 954.

26. K. Deplanche, M. L. Merroun, M. Casadesus, D. T. Tran, I. P. Mikheenko, J. A.Bennett, J. Zhu, I. P. Jones, G. A. Attard, J. Wood, S. S. Pobell and L.E. Macaskie, *J. R. Soc. Interface,* 2012, **9**, 1705.

27. Y. W. Lee, M. Kim, Z. H. Kim and S. W. Han, *J. Am. Chem. Soc.,* 2009, **131**, 17036.

28. L. Lu, H. Wang, S. Xi and H. Zhang*, J. Mater. Chem.,* 2002, **12**, 156.

29. H. Chen, G. Wei, A. Ispas, S. G. Hickey and A. Eychmüller, *J. Phys. Chem. C*, 2010, **114**, 21976.

30. N. Toshima and T. Yonezawa, *New J. Chem.*, 1998, **22** 1179.

31. L. Chen, C. Wan and Y Wang, *J. Colloid Interface Sci.,* 2006, **297**, 143.

32. Z. Borkowska, A. T. Zielinska and G. Shul, *Electrochim. Acta,* 2004, **49**, 1209.

33. A. S. Aarnio, Y. Kwon, E. Ahlberg, K. Kontturi, T. Kallio and M. T. M. Koper, *Electrochem. Commun.,* 2011, **13**, 466.

34. Y. Su, M. Zhang, X. Liu, Z. Li, X. Zhu, C. Xu and S. P. Jiang, *Int. J. Electrochem. Sci.,* 2012, **7**, 4158.

35. X. Y. Lang, H. Guo, L. Y. Chen, A. Kudo, J. S. Yu, W. Zhang, A. Inoue and M. W. Chen, *J. Phys. Chem. C,* 2010, **114**, 2600.

36. A. V. Tripkovic, K. Dj. Popovic, J.D. Lovic, V. M. Jovanovic and A. Kowal, *J.Electroanal. Chem.*, 2004, **572**, 119.

37. A. V. Tripkovic, K. D. Popovic and J. D. Lovic, *J. Serb. Chem. Soc.,* 2007, **72**, 1095.

38. W. P. Zhou, A. Lewera, R. Larsen, R. I. Masel, P. S. Bagus and A. Wieckowski, *J. Phys. Chem. B*, 2006, **110**, 13393.

39. V. Mazumder and S. Sun, *J. Am. Chem. Soc.*, 2009, **131**, 4588.

40. R. Manoharan and J. B. Goodenough, *J. Mater. Chem.*, 1992, **2**, 875.

41. K. Kunimatsu, *J. Electroanal. Chem.*, 1983, **145**, 219.

42. D. Wang, J. Liu, Z. Wu, J. Zhang, Y. Su, Z. Liu and C. Xu, *Int. J. Electrochem. Sci.*, 2009, **4**, 1672; O. O. Fashedemi and K. I. Ozoemena, *Phys. Chem. Chem. Phys.*, 2013, **15**, 20982; V. Bambagioni, C. Bianchini, A. Marchionni, J. Filippi, F. Vizza, J. Teddy, P. Serp and M. Zhiani, *J. Power Sources,* 2009, **190**, 241; L. Yang, W. Yang and Q. Cai, *J. Phys. Chem. C,* 2007, **111**, 16613.

43. M. I. Manzanares, A. G. Pavese and V. M. Solis, *J. Electroanal. Chem.*, 1991, **310**, 159.

44. T. Takamura and Y. Sato, *Electrochim. Acta,* 1974, **19**, 63.

45. J. L. Davis and M. A. Barteau, *Surface Sci.,* 1987, **187,** 387.

46. K. Franaszczuk, E. Herrero, P. Zelenay, A. Wieckowski, J. Wang and R. I. Masel, *J. Phys. Chem. ,* 1992, **96**, 8509.

47. J. S. Spendelow, J. D. Goodpaster, P. J. A. Kenis and A. Wieckowski, *Langmuir,* 2006, **22**, 10457.

48. K. A. Assiongbon, D. Roy, *Surface Sci.,* 2005, **594**, 99.

49. S. T. Oyama, R. Radhakrishnan, M. Seman, J. N. Kondo, K. Domen and K. Asakura, *J. Phys. Chem. B,* 2003, **107**, 1845.

50. Y. Kwon, S. C. S. Lai, P. Rodriguez and M. T. M. Koper, *J. Am. Chem. Soc.*, 2011, **133**, 6914.

51. S. Lj. Gojkovic, T. R. Vidakovic and D. R. Durovic, *Electrochim. Acta*, 2003, **48**, 3607.

52. R. K. Pandey and V. Lakshminarayanan, *J. Phys. Chem. C,* 2010, **114**, 8507.

53. J. S. Spendelow and A. Wieckowski, *Phys. Chem. Chem. Phys.*, 2007, **9**, 2654.

54. R. C. Sekol, M. Carmo, G. Kumar, F. Gittleson, G. Doubek, K. Sun, J. Schroers and A.D. Taylor, *Int. J. Hydrogen Energy*, 2013, **38**, 11248.

Journal of Materials Chemistry A Accepted Manuscript

One step preparation of 'ready to use' Au@Pd nanoparticle modified surface using Deep eutectic solvents and a study of its electrocatalytic properties in methanol oxidation reaction.

Anu Renjith, Lakshminarayanan V.*
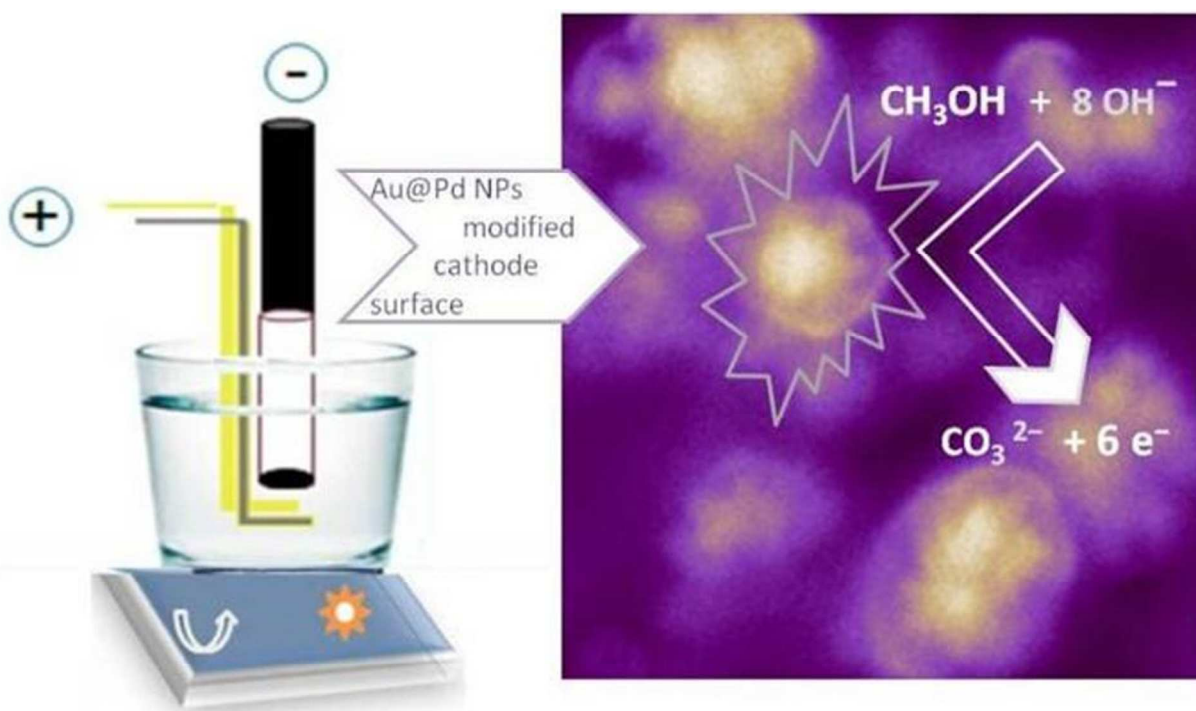
A facile one pot synthesis and *insitu* electrodeposition of Au-Pd core shell nanoparticles (Au@Pd NPs) could be achieved in a deep eutectic solvent. The fabricated Au@Pd NPs modified graphite showed superior electrocatalytic properties for methanol oxidation at low activation energies.